Simultaneous Interpolation of 4 Spatial Dimensions

Bin Liu and Mauricio D. Sacchi, Department of Physics, University of Alberta, Daniel Trad, Veritas DGC Inc.*

Summary

In this article we propose an interpolation scheme for prestack 3-D data. In particular, we have extended the Minimum Weighed Norm Interpolation (MWNI) method proposed by Liu and Sacchi (2001) to interpolate data that depend on 4 spatial dimensions.

The method is tested with a field data example from the Western Canadian Sedimentary Basin (WCSB).

Introduction

The Minimum Weighted Norm Interpolation (MWNI) algorithm (Liu and Sacchi, 2001) has been proposed as a method to reconstruct band-limited seismic data along 1, 2 and 3 spatial dimensions. In addition, tests showing the ability of the method to reconstruct data prior to amplitude versus angle wave equation migration were provided in Liu et. al (2003). The method incorporates bandwidth limitation constraints, and a spectral smoothness constraint that becomes a key feature of the algorithm at the time of interpolating large segments of missing information.

Multi-dimensional MWNI

The complete unknown data x and the incomplete measurements y are related via the following expression

$$\mathcal{T} x = y \tag{1}$$

where $\mathcal{T}$ is the sampling operator or mask function with entries given by

$$T_{ij} = \begin{cases} 1 & \text{if } i\,j \text{ contains an observation} \\ 0 & \text{if } i\,j \text{ is a pixel/bin with missing information.} \end{cases} \tag{2}$$

The complete data x can be retrieved by minimizing the following cost function:

$$J = ||\mathcal{T} x - y||_2^2 + \mu x^T \, Q^\dagger \, x \tag{3}$$

where the matrix of weights Q is given by the following expression:

$$Q^\dagger \; = \; \mathcal{F}_{ND}^H \, \Lambda^\dagger \, \mathcal{F}_{ND} \, , \tag{4}$$

$\mathcal{F}_{ND}$ and $\mathcal{F}_{ND}^H$ symbolize forward and inverse ND Fourier transforms, respectively. The band-limiting operator $\Lambda^\dagger$ is given by

$$\Lambda^\dagger(\mathbf{k}) \; = \; \begin{cases} [S(\mathbf{k})]^{-1} & [\mathbf{k}] \in \Omega(\mathbf{k}) \\ 0 & [\mathbf{k}] \notin \Omega(\mathbf{k}) \end{cases} \tag{5}$$

where $S(\mathbf{k})$ is the unknown spectral density of the multidimensional prestack data cube and $\Omega(\mathbf{k})$ denotes the region of spectral support. The wavenumber vector is indicated by $\mathbf{k}$. In our problem the wavenumber vector is defined as $\mathbf{k} = [k_{sx}, k_{sy}, k_{gx}, k_{gy}]^T$, where (sx, sy) indicates the inline and crossline source coordinate and (gx, gy) the inline and crossline geophone coordinate. We will assume that the data are band-limited. In other words, $S(\mathbf{k}) = 0 \, , \in \bar{\Omega}(\mathbf{k})$, the complement of $\Omega(\mathbf{k})$.

The cost function given by equation (3) is minimized using the method of conjugate gradients. In our numerical implementation we have reduced the cost function to its standard form (Hansen, 1998) and use the so called *regularization by iteration* method (Hanke, 1995). After the following change of variables

$$x = \mathcal{W} \, z \tag{6}$$

the cost function (in the standard form) becomes

$$J = ||\mathcal{T} W z - y||_2^2 + \mu z^T \, z \tag{7}$$

where

$$W(\mathbf{k}) \; = \; \begin{cases} [S(\mathbf{k}]^{1/2} & \mathbf{k} \in \Omega(\mathbf{k}) \\ 0 & \mathbf{k} \notin \Omega(\mathbf{k}) \end{cases} \; . \tag{8}$$

Equation (7) is solved using conjugate gradients with regularization by iteration. This is equivalent to finding the smallest number of iterations n that satisfies the discrepancy principle: $||\mathcal{T} W z^n - y||_2^2 \approx \epsilon$.

The forward and adjoint operators required by the CG method are given by:

Forward:
$\mathcal{T} W x =$ `sampling (ifft (filtering ( fft(x)))`
Adjoint:
$W' \mathcal{T}' \, y =$ `ifft (filtering ( fft (sampling(y)))`

where `sampling` entails applying the operator $\mathcal{T}$, `filtering` represents wavenumber domain multiplication with the operator W, `fft` and `ifft` denote the ND Fast Fourier Transform and Inverse FFT, respectively. It is clear that a simple *in the flight* implementation leads to a very efficient algorithm.

Estimation of $S(\mathbf{k})$

The algorithm outlined above requires the knowledge of the power spectral density (PSD) of the complete data x. This is an unknown and, therefore, it will be bootstrapped from the available data. The spectral density is computed via the following algorithm:

1 Define W as an initial multi-dimensional band-limiting operator.
2 Use CG to solve $\mathcal{T}Wz \approx y$, and obtain an initial reconstruction of the data $\hat{x} = W\hat{z}$
3 Re-estimate the PSD from the reconstructed data $\hat{x}$, and compute $W(\mathbf{k})$ using equation (8).
4 Repeat steps 2 and 3 until achieving convergence.

Examples

2-D Example [`SeaBeam Data Set`]: This example also portrayed in Fomel and Clearbout (2003) is used to illustrate the importance of spectral weights at the time of reconstructing sparse images (data). The `SeaBeam` system is used to measure water depth under and somewhat off the sides of the ship's track. An interpolation scheme can be tested by its ability to hide acquisition footprints. In Figure 1A we provide the evolution of the MWNI algorithm after each iteration. In our simulation convergence was attained after 15 iterations. The initial PSD of the data (Figure 1B) and the final estimator of the PSD (Figure 1C) are also provided. The initial PSD utilized in this exercise is a 2D isotropic separable Kaiser window. The solution at the first iteration is also the solution we would have obtained by applying band-limiting constraints only. It is clear that band-limiting constraints are not sufficient at the time of reconstructing large portions of missing observations.

4-D Example [`WCSB`]: The 4D MWNI algorithm is used to interpolate a multi-azimuth 3D land dataset from the Western Canadian Sedimentary basin. The dataset was acquired using the MegaBin acquisition scheme. The shot and receiver geometry of the dataset is illustrated in Figure 2A and 2C, respectively. The original shot spacing along the inline and crossline direction is 140 m. The receiver spacing is 70 m along the inline direction and 140 m along the crossline direction. Note that many shots and receivers are missing in the real geometry. The shot and receiver geometry of the interpolated output is shown in Figure 2B and 2D, respectively. Note that after interpolation, the shot spacing along the inline direction is reduced to 70 m and the shot spacing along the crossline direction remains the same, and both inline and crossline receiver spacings are reduced to 35 m. Before interpolation, the data have been datumed to the same depth. The interpolation began by dividing the whole survey area into many sections, the 4D MWNI is applied along sx, sy, gx, gy coordinates in each section. Figure 2E shows the output shot geometry in one section. There are approximately 8×8 shots in each section. Figure 3A and 3B show a comparison of inline receivers before (Figure 3A) and after (Figure 3B) interpolation. Crossline receivers before and after interpolation are shown in Figure 3C and 3D, respectively. Figure 4A and 4B show a comparison of inline receivers before (Figure 4A) and after (Figure 4B) interpolation where the NMO correction has been applied before interpolation to reduced the wavenumber bandwidth. Crossline receivers before and after interpolation with the NMO correction are shown in Figure 4C and 4D, respectively. Finally, Figure 5A and Figure 5B show a comparison of a time slice of the final stack before and after the interpolation. Notice the improved spatial resolution in the stack with the interpolation.

Conclusions

In this abstract, we applied the minimum weighted norm interpolation algorithm to interpolate 3D prestack data. In particular, a 4D MWNI scheme has been successfully applied to interpolate a multi-azimuth field dataset from WCSB.

The MWNI method permits one to incorporate the a priori spectral signature (band-width and the signal spectrum shape) of the unknown wavefield and is efficiently implemented with a preconditioned CG scheme. The computational efficiency makes it attractive to interpolate large 3D prestack datasets and to deal with higher dimensional interpolation problems where other interpolation methods do not have a straighforward implementation.

References

Liu B. and Sacchi M. D., 2001, Minimum weighted norm interpolation of seismic data with adaptive weights: 71st Ann. Internat. Mtg., Soc. of Expl. Geophys., Expanded Abstracts, 1921–1924.

Liu, B., Sacchi, M. D. and Kuehl, H., 2003, 2D/3D seismic wavefield reconstruction for AVA imaging, 73rd Ann. Internat. Mtg.: Soc. of Expl. Geophys., 235-238.

Hanke, M., 1995, Conjugate Gradients Type Methods for Ill-posed problems: Longmand Scientific and Technical.

Hansen, P. C., 1998, Rank-Deficient and Discrete Ill-Posed Problems: SIAM.

Fomel, S. and Claerbout, J. F., 2003, Multidimensional recursive filter preconditioning in geophysical estimation problems: Geophysics, **68**, 577-588.

Acknowledgments

We thank Alistair Harding (UCSD) and Jon Claerbout (Stanford University) for providing the SeaBeam data and interesting discussions on the interpolation problem. We acknowledge Scott Cheadle and Murry Desjarlais from Veritas Geoservices for their contributions to the WCSB project. Special thanks to Heather Joy and The Encana Corporation for providing the field data and supporting the project.

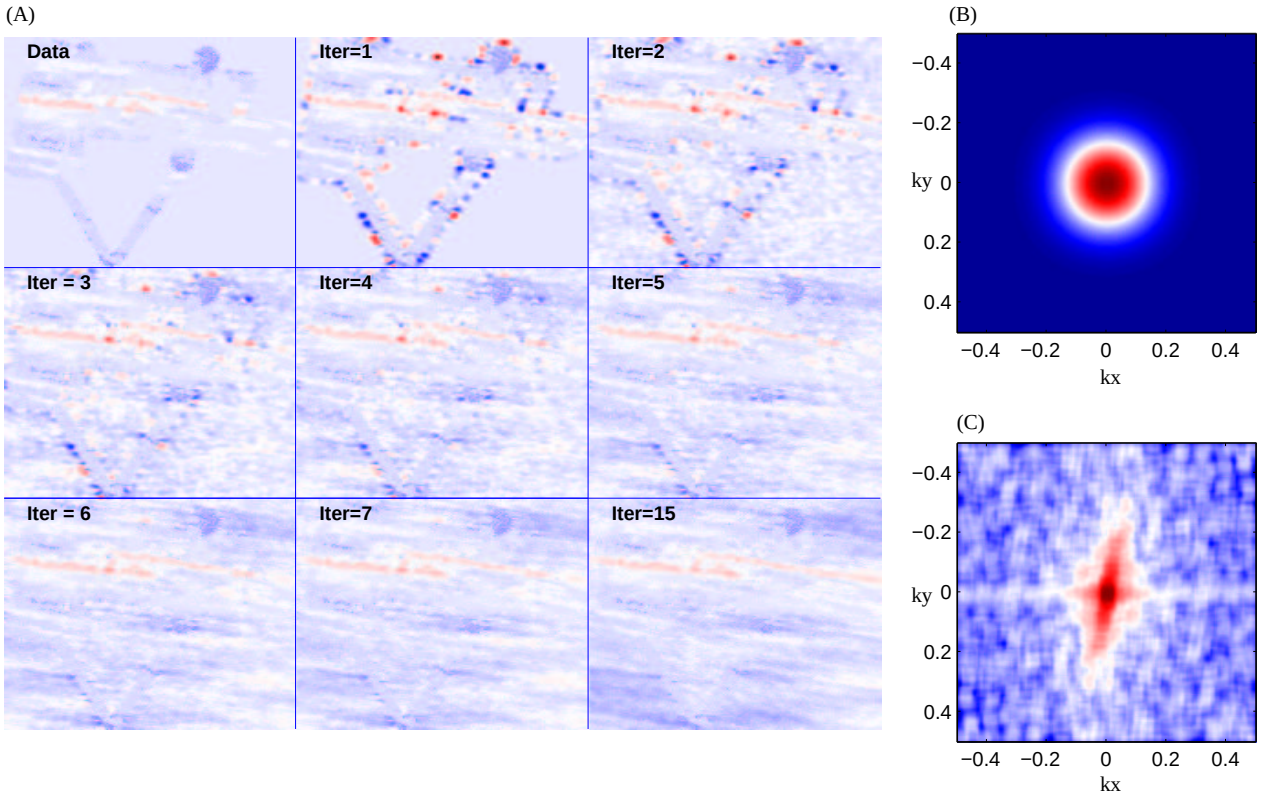

Fig. 1: (A) Evolution of the MWNI algorithm after each iteration where convergence was attained after 15 iterations. (B) The 2D isotropic separable Kaiser window used for the initial PSD of the data. (C) The final estimator of the PSD.

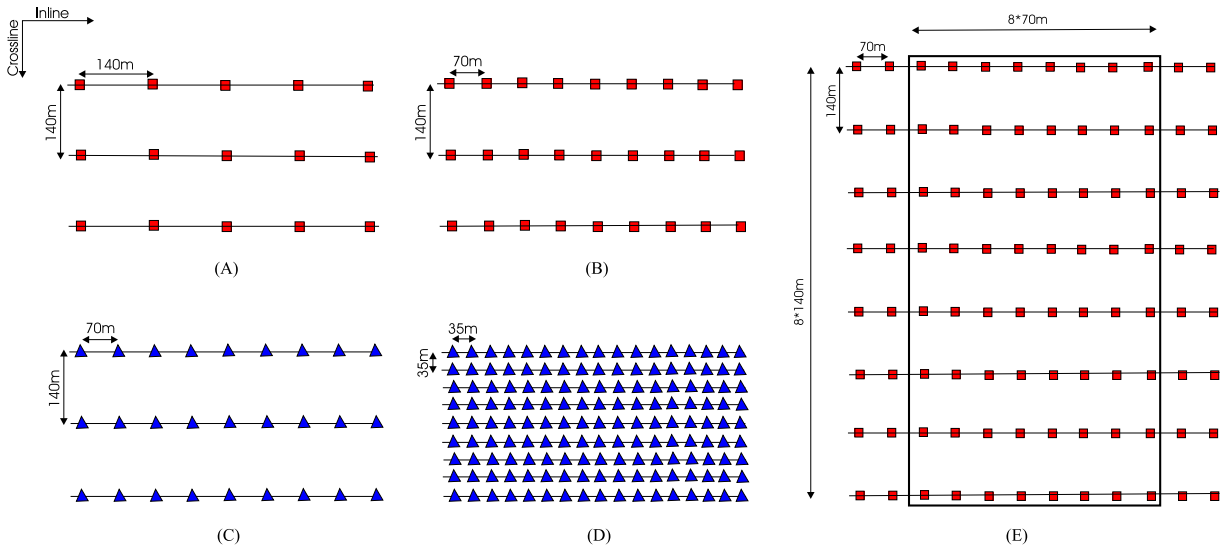

Fig. 2: The input and output geometry of the 4D interpolation. (A) The original shot geometry. (B) The output shot geometry. (C) The original receiver geometry. (D) The output receiver geometry. (E) The output shot geometry in one section of the interpolation.

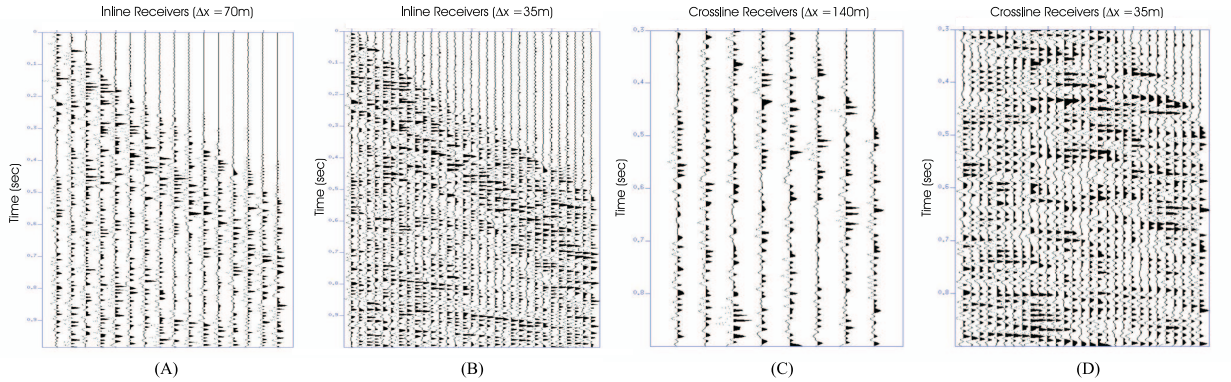

Fig. 3: Interpolation of inline and crossline receivers without NMO (Zoomed). (A) Original inline receivers with a sampling interval of 70m. (B) Interpolated inline receivers with a sampling interval of 35m. (C) Original crossline receivers with a sampling interval of 140m. (D) Interpolated crossline receivers with a sampling interval of 35m.

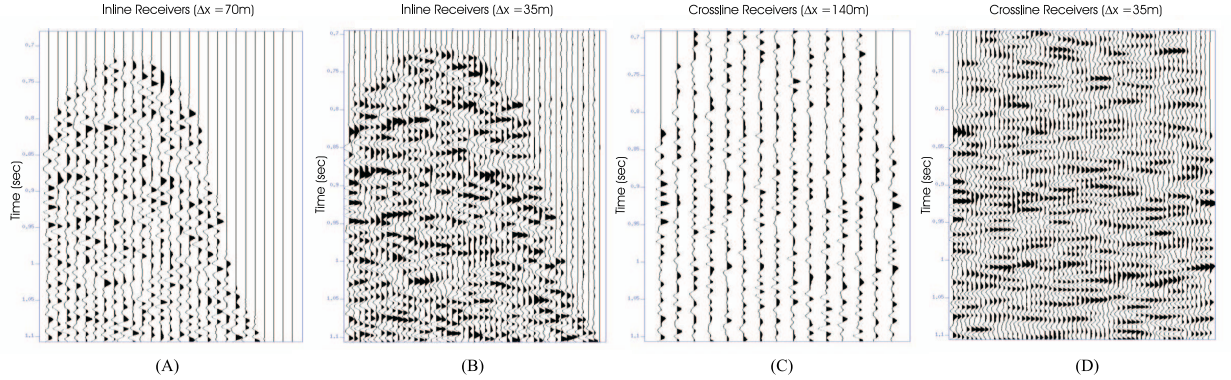

Fig. 4: Interpolation of inline and crossline receivers with NMO (Zoomed). (A) Original inline receivers with a sampling interval of 70m. (B) Interpolated inline receivers with a sampling interval of 35m. (C) Original crossline receivers with a sampling interval of 140m. (D) Interpolated crossline receivers with a sampling interval of 35m.

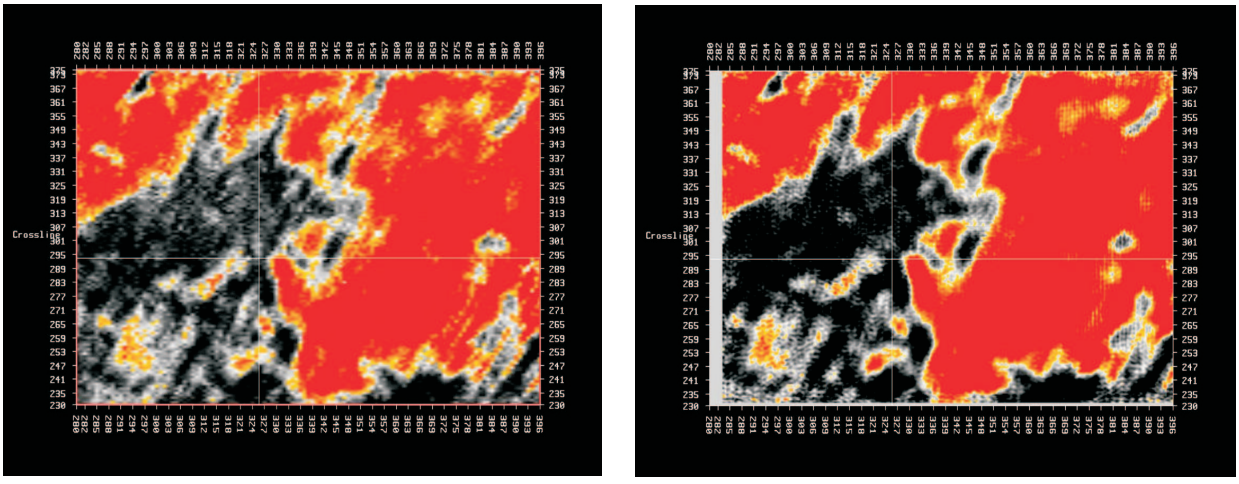

Fig. 5: A time slice of the final stack without interpolation (A) and with interpolation (B).